Design of cascaded plasmon resonances for ultrafast nonlinear optical switching

S. Toroghi*[,a], P. G. Kik[a,b]
[a]CREOL, The College of Optics and Photonics, University of Central Florida, 4000 Central Florida Blvd, Orlando, FL 32816, USA
[b]Department of Physics, University of Central Florida, 4000 Central Florida Blvd, Orlando, FL 32816, USA

ABSTRACT

The optical properties of cascaded plasmon resonant metallic nanocomposites are investigated. Plasmon resonances and their related field distributions are numerically evaluated in two-dimensional arrays of spherical silver nanoparticles embedded in a dielectric host. The field distributions in structures with identical particle sizes indicate the presence of a largely dipolar particle response, with a small multipole resonance contribution at high frequency. However, in arrays consisting of particles with dissimilar sizes, an additional coupled mode appears in which the dipole moment in adjacent particles is found to be anti-parallel. For increasing size-dissimilarity a higher electric field enhancement is observed inside the small metal nanospheres, indicative of a cascaded field enhancement effect. This effect may be used to enhance the nonlinear optical response of an effective medium composed of particles with engineered size dispersion and particle placement.

Keywords: Cascaded plasmon resonance, metallic nanocomposites, nonlinear optics, optical switching

1. INTRODUCTION

Plasmon resonant metal-dielectric nanocomposites have attracted a tremendous amount of attention due to their ability to induce strongly enhanced local electric fields. Plasmon enhanced local electric fields can dramatically increase the nonlinear optical response of nanocomposites, which can be used for example in all-optical switching and nonlinear optical absorption elements [1,2].

While isolated plasmon resonant nanospheres support significant field enhancement, Li and co-workers [3] demonstrated that additional field enhancement can be achieved in a self-similar chain of nanoparticles, an effect that was referred to as a nanolens. They showed that a finite number of nanoparticles with proper separations and sizes can produce a high local field enhancement in a specific location and frequency. The effect can be understood as a cascading of plasmon resonances, in which the enhanced field around a large plasmon resonant nanoparticle is used to excite a smaller particle that is resonant at the same frequency, leading to multiplicative field enhancement. Recently, Kravets and co-workers [4] used a structure with three coaxial gold nanodiscs with different diameters on top of each other to show the cascaded field enhancement effect experimentally. Both studies focused on the magnitude of the resulting field enhancement in order to improve applications such as surface enhanced Raman scattering (SERS), while the phase and distribution of the fields received less attention. The latter two factors are in fact vital in the enhancement of Kerr-type nonlinear optical response [5-9].

This paper studies effective media consisting of infinite chains of coupled spherical silver nanoparticles with dissimilar sizes in order to evaluate cascaded plasmon resonances and their related field distributions in metallic nanocomposites. The linear optical properties of structures with a binary size distribution are studied as a function of particle size dissimilarity. We monitor the development of coupled resonances, and investigate the corresponding electric field distributions. Clear evidence for cascaded field enhancement is presented as the size dissimilarity is increased. It is shown that the significant increase in field enhancement is accompanied by a much smaller increase of the linear absorption of the composite. This observation implies the possibility of achieving a large enhancement of the nonlinear optical response without introducing additional linear loss, promising the design of structures and devices with improved figure of merit.

*storoghi@creol.ucf.edu

Enabling Photonics Technologies for Defense, Security, and Aerospace Applications VII, edited by Michael J. Hayduk, Peter J. Delfyett, Jr., Proc. of SPIE Vol. 8054, 80540E · © 2011 SPIE · CCC code: 0277-786X/11/$18 · doi: 10.1117/12.884045

2. SIMULATION GEOMETRY

We consider infinite two dimensional arrays of closely spaced spherical silver nanoparticles embedded in a host with a frequency independent real refractive index of 1.5. Three-dimensional frequency domain electromagnetic simulations were performed using CST Microwave Studio [10]. To simulate the structure, a rectangular section of the unit cell with dimensions L_x, L_y, L_z given by 30 nm, 70 nm and 100 nm was considered as indicated by the dashed line in Fig. 1. By applying electric ($E_{//}$=0) and magnetic ($H_{//}$=0) boundary conditions respectively on the y-z bounding planes and the x-z bounding planes of the simulation volume the periodic structure in Fig. 1 is reproduced. Open boundary conditions are used along the z-direction. The center-to-center spacing between adjacent nanoparticles is set to 30 nm along the x-direction in all simulations. The structure is excited using a plane wave propagating in the z-direction and polarized along the x-direction. The inter-particle spacing along the x- and y-directions is smaller than the shortest optical wavelength considered in the host, and consequently diffractive effects do not affect the optical properties of these composites. The size of the silver nanospheres is alternated periodically along the array, and the relative volume of the two types of particles with radii R_1 and R_2 is varied while maintaining a fixed fill fraction of 1%. Structures with five different volume ratios $(R_2/R_1)^3$ are simulated, with volume ratio values of 1 (identical particles), 2.3, 4.8, 11 and 30.

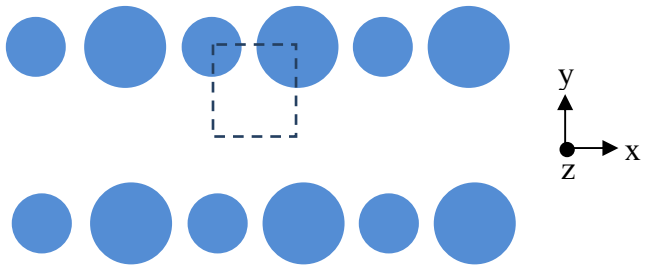

Figure 1. Top view of a representative simulated cascaded plasmon resonant structure, consisting of periodic arrays of silver nanoparticles with alternating particle size. The dashed rectangle shows the simulated region.

The silver dielectric function is described by a Drude model fit to literature data given by $\varepsilon_{Ag} = \varepsilon_\infty - \omega_p^2/(\omega^2 + i\omega\Gamma)$ where $\varepsilon_\infty = 5.451$, $\omega_p = 1.474 \times 10^{16}$ rad/s, and the electron scattering rate is $\Gamma = 8.354 \times 10^{13}$ s^{-1}. For simplicity surface scattering is neglected in these simulations. The maximum error in the fitted dielectric function compared to the experimental values is ± 0.2 for real part and ± 0.14 for imaginary part in the simulated wavelength range of 360-500 nm.

3. RESULTS

Figure 2 shows the frequency dependent phase and amplitude of E_x (field component along the nanoparticle chain) at the center of one of the small nanoparticles, for the five different volume ratios simulated. One dominant resonant mode is observed for the structure with identical nanoparticle volume (red curve). For this structure, the phase of the internal electric field in the nanoparticle is seen to increase by approximately π radians as the incident wavelength is decreased, similar to the response of an isolated Lorentz resonator. For structures with two different particle sizes, an additional peak is seen to appear in the electric field amplitude inside the small nanoparticle. Phase shifts are seen to occur at frequencies at frequencies near and above this additional peak. The field amplitude in the small particle is seen to increases at frequencies close to both resonances as the size dissimilarity is increased, indicative of a cascaded resonance effect.

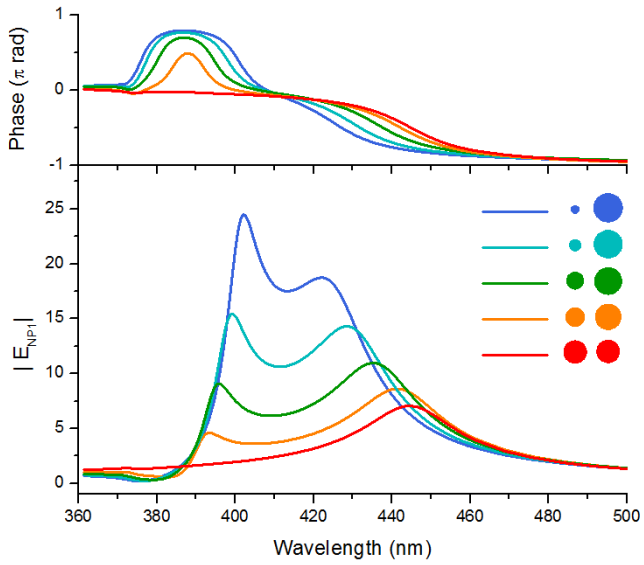

Figure 2. a) Phase and b) amplitude of the x-component of the electric field inside the small nanoparticle for five different structures with relative particle volumes of 1, 2.3, 4.8, 11, 30.

Figure 3 shows the phase and the amplitude of the x-component of the electric field at the center of the large nanoparticles for every structure. The red curve shows the results in a structure with identical particle sizes, and is therefore identical to the red curve in Fig. 2. In structures with dissimilar nanoparticle sizes, two peaks are observed in the x-component of the electric field amplitude in the large particles. The variation of the maximum field strength of the low frequency peak is less than 1 V/m for the different investigated structures, showing that the cascading phenomenon has a relatively minor effect on the larger particles, even though it was shown to dramatically affect the field in the smaller particles. The phase shift related to the low frequency peak is almost π radian in all simulations, similar to the phase shift observed in the small nanoparticle around this resonance. In structures with dissimilar particle sizes, additional phase shifts are seen to occur at frequencies close to the high frequency peak.

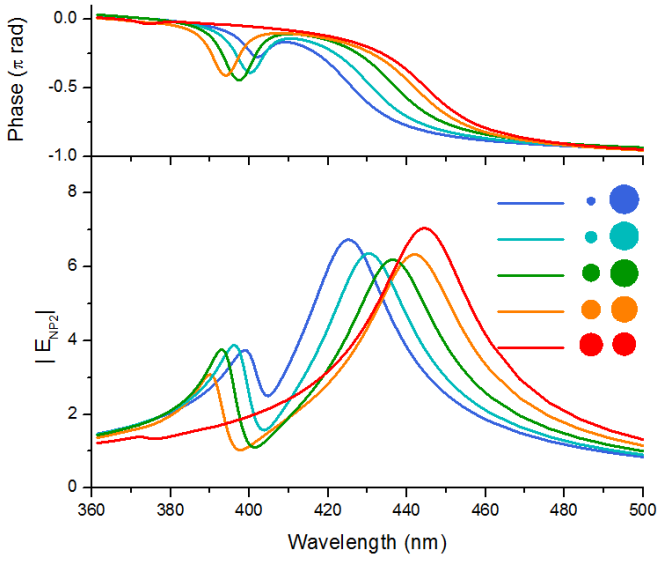

Figure 3. a) Phase and b) amplitude of the x-component of the electric field inside the large nanoparticle for five different structures with relative particle volumes of 1, 2.3, 4.8, 11, 30.

In a composite that contains multiple isotropic materials *j* with frequency-dependent dielectric function $\varepsilon_j(\omega)$, illuminated by a plane wave polarized along one of the main symmetry axes of the composite (here the x-direction) the effective dielectric constant $\varepsilon_c(\omega)$, can be found through integration of simulated electric field distributions according to [11]

$$\varepsilon_c(\omega) = \frac{\langle \varepsilon_j(\omega)\, \vec{E}(\omega,\vec{r})^2 \rangle_{V_j}}{\langle \vec{E}(\omega,\vec{r}) \rangle_V^2} \qquad (1)$$

Note that ε_c here represents the ε_{xx} tensor component of the dielectric function in our anisotropic structure. The notation $< >_V$ represents spatial averaging over the simulation volume V, and $< >_{Vj}$ represents spatial averaging of the volume occupied by material *j*. The quantity $\vec{E}(\omega,\vec{r})$ is the complex electric field amplitude at position $\vec{r}$ and at frequency ω. Equation (1) is used to calculate the linear absorption spectra for different structures based on the simulated three-dimensional electric field data. Figure 4 shows the thus obtained linear absorption spectra for the five different simulated structures. All structures exhibit clear absorption resonances at frequencies close to the resonance peaks observed in the internal electric field (Figures 2 and 3). Note that the resonances near 400 nm lead to a relatively weak absorption, despite the strong field enhancement observed in Fig. 2. This can be understood by realizing that the volume over which the enhanced field is present is gradually reduced as the size dissimilarity is increased. In addition, a previously unobserved high frequency resonance appears in the absorption spectra at wavelengths close to 375 nm (see inset in Fig. 4).

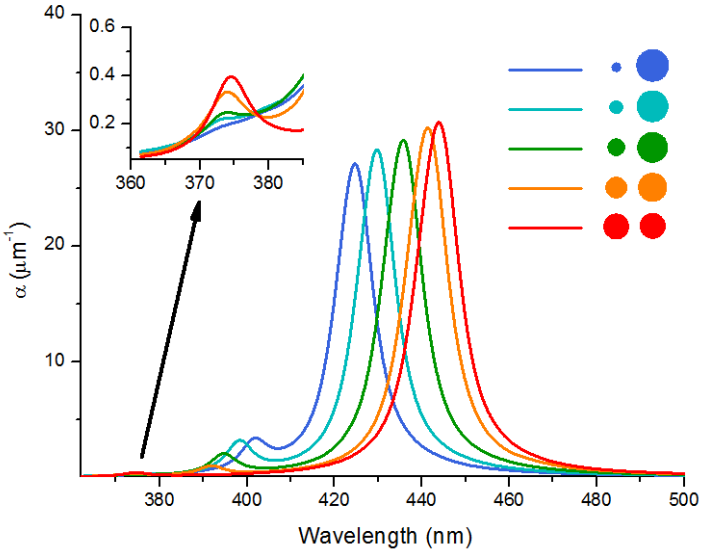

Figure 4. Absorption spectrum of the five periodic nanostructures with different particle size dissimilarity. The inset shows a magnified view of a weak high-frequency absorption feature.

To understand the nature of the peaks in the linear absorption spectra, the electric field distributions in representative structures are considered at several key frequencies. Relative particle volumes $(R_2/R_1)^3$ of 1, 4.8 and 30 are considered. Figure 5 shows the electric field distribution for the three different structures at wavelengths of 444 nm, 438 nm and 423 nm respectively, corresponding to the spectral location of the main absorption peak. All structures show significant field enhancement in and near the nanoparticles. Note that the electric field in each nanoparticle is positive at the phase shown. This resonance will be labeled the 'symmetric' mode, since the dipole moment of adjacent particles is parallel. As the size dissimilarity increases, the field strength in the small particle is seen to increase, while the field strength in the larger particle remains approximately constant, in correspondence with the results shown in Fig. 2 and Fig. 3.

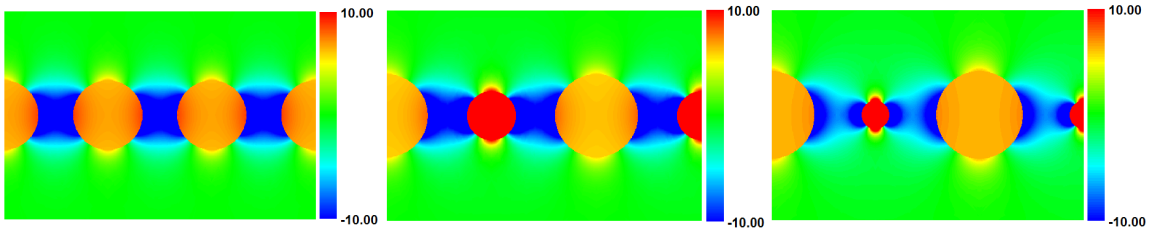

Figure 5. Distribution of the x-component of the electric for the main low frequency absorption peak, shown for relative particle volumes of a) 1, b) 4.8 and c) 30. This mode corresponds to a predominantly dipolar plasmon resonance in the individual nanoparticles, with the direction of the dipole moment in adjacent particles aligned in parallel. This mode is labeled the symmetric mode.

Figure 6 shows the distribution of the x-component of the electric field for structures with a volume ratio of 4.8 and 30 at a wavelength of 397 nm and 403 nm respectively. These wavelengths correspond to the location of the additional absorption peak that was seen to develop in structures with dissimilar particle sizes (Fig. 4). This mode does not appear in the structure with a single nanoparticle size. Note that the electric field in adjacent particles is antiparallel. This mode will be referred to as the antisymmetric mode. The field distribution can be seen to exhibit a partial multipolar character.

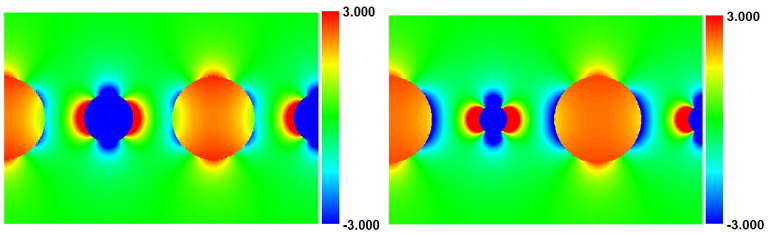

Figure 6. The distribution of the x-component of the electric field in structures with relative particle volumes of a) 4.8 and b) 30 at wavelengths of 397 nm and 403nm respectively.

Figure 7 shows the electric field distribution for the weak high frequency absorption peaks observed at wavelengths near 375nm for different relative particle volumes of 1, 4.8 and 30 respectively. All corresponding field distributions are seen to be predominantly multipolar. While these multipole modes are not typically excited with significant amplitude in particles much smaller than the incident wavelength, the proximity of neighboring particles leads to the presence of inhomogeneous near fields which allow the excitation of higher order plasmon resonance modes.

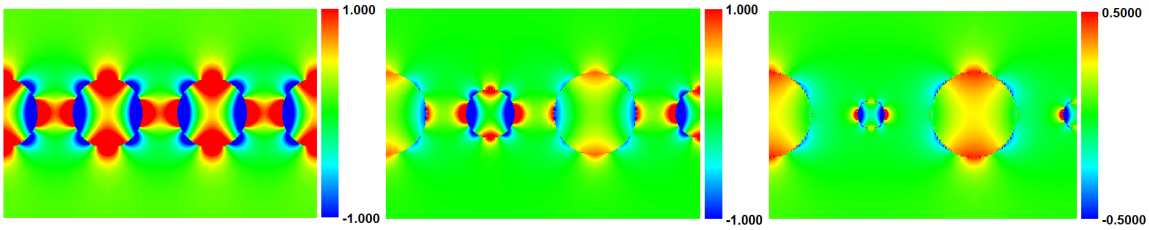

Figure 7. The distribution of the x-component of the electric field for the high frequency mode observed at a wavelength of 375 nm for three different structures with relative particle volumes of a) 1, b) 4.8 and c) 30.

4. SUMMARY

The absorption spectra of five different cascaded plasmon resonance structures are calculated using a combination of numerical simulation and effective medium theory. The nature of the different resonance peaks of different structures is investigated by analyzing the electric field distributions excited on the nanoparticles. Clear symmetric and antisymmetric collective resonances are observed in the structures, as well as a much weaker multipolar resonance peak. The electric field enhancement inside the smaller nanospheres in the cascaded structures is found to increase by a factor ~3 (for the symmetric mode) and ~10 (for the antisymmetric mode) as the size dissimilarity is increased, while the maximum absorption at the corresponding frequencies is relatively unaffected. These results suggest that an enhanced nonlinear optical response can be obtained in these structures, without significantly reducing the transparency of the composite. This implies the possibility of achieving improved figures of merit for device performance in devices based on these types of structures.

ACKNOWLEDGMENT

This material is based upon work supported by the U. S. Army Research Office under contract/grant number 50372-CH-MUR.

REFERENCES

[1] Min, C., Wang, P., Chen, C., Deng, Y., Lu, Y., Ming, H., Ning, T., Zhou, Y. and Yang, G., "All-optical switching in subwavelength metallic grating structure containing nonlinear optical materials," Opt. Lett. 33(8), 869–871 (2008).

[2] Kiran, P. P., Bhaktha, B. N. S., Rao, D.N. and De, G., "Nonlinear optical properties and surface plasmon enhanced optical limiting in Ag–Cu nanoclusters co-doped in SiO_2 sol-gel films," J Appl Phys 96, 6717–6723, (2004).

[3] Li, K. R., Stockman, M. I. and Bergman, D. J., "Self-similar chain of metal nanospheres as an efficient nanolens," Phys. Rev. Lett. 91, 227402 (2003).

[4] Kravets, V. G., Zoriniants, G., Burrows, C. P., Schedin, F., Casiraghi, C., Klar, P., Geim, A. K., Barnes, W. L. and Grigorenko, A. N., "Cascaded Optical Field Enhancement in Composite Plasmonic Nanostructures," Phys. Rev. Lett. 105, 246806 (2010).

[5] Sipe, J. E. and Boyd, R. W., "Nonlinear susceptibility of composite optical materials in the Maxwell Garnett model," Phys. Rev. A 46(3), 1614–1629 (1992).

[6] Smith, D. D., Fischer, G., Boyd, R. W. and Gregory, D. A., "Cancellation of photoinduced absorption in metal nanoparticle composites through a counterintuitive consequence of local field effects," J. Opt. Soc. Am. B 14(7), 1625–1631 (1997).

[7] Stockman, M. I., Kurlayev, K. B. and George, T. F., "Linear and nonlinear optical susceptibilities of Maxwell Garnett composites: Dipolar spectral theory," Phys. Rev. B 60(24), 17071–17083 (1999).

[8] Piredda, G., Smith, D. D., Wendling, B. and Boyd, R. W., "Nonlinear optical properties of a gold-silica composite with high gold fill fraction and the sign change of its nonlinear absorption coefficient," J. Opt. Soc. Am. B 25(6), 945–950 (2008).
[9] Kohlgraf-Owens, D. C. and Kik, P. G., "Structural control of nonlinear optical absorption and refraction in dense metal nanoparticle arrays," Opt. Express 17, 15032–15042 (2009).
[10] CST MICROWAVE STUDIO® 2009, Computer Simulation Technology, Darmstadt, Germany.
[11] Levy, O. and Stroud, D., "Maxwell Garnett theory for mixtures of anisotropic inclusions: Application to conducting polymers," Phys. Rev. B 56(13), 8035–8046 (1997).